Persistent Binding of MgADP to the E187A Mutant of *Escherichia coli* Phosphofructokinase in the Absence of Allosteric Effects†

Audrey S. Pham,*,‡ Fabiola Janiak-Spens,§ and Gregory D. Reinhart||

Division of Pathology and Laboratory Medicine, The University of Texas M. D. Anderson Cancer Center, Houston, Texas 77030, Department of Chemistry and Biochemistry, University of Oklahoma, 620 Parrington Oval, Norman, Oklahoma 73019, and Department of Biochemistry and Biophysics, Texas A&M University, College Station, Texas 77843

Received July 28, 2000; Revised Manuscript Received January 24, 2001

ABSTRACT: MgADP binding to the allosteric site enhances the affinity of *Escherichia coli* phosphofructokinase (PFK) for fructose 6-phosphate (Fru-6-P). X-ray crystallographic data indicate that MgADP interacts with the conserved glutamate at position 187 within the allosteric site through an octahedrally coordinated Mg^{2+} ion [Shirakihara, Y., and Evans, P. R. (1988) *J. Mol. Biol. 204*, 973−994]. Lau and Fersht reported that substituting an alanine for this glutamate within the allosteric site of PFK (i.e., mutant E187A) causes MgADP to lose its allosteric effect upon Fru-6-P binding [Lau, F. T.-K., and Fersht, A. R. (1987) *Nature 326*, 811−812]. However, these authors later reported that MgADP inhibits Fru-6-P binding in the E187A mutant. The inhibition presumably occurs by preferential binding to the inactive (T) state complex of the Monod−Wyman−Changeux two-state model [Lau, F. T.-K., and Fersht, A. R. (1989) *Biochemistry 28*, 6841−6847]. The present study provides an alternative explanation of the role of MgADP in the E187A mutant. Using enzyme kinetics, steady-state fluorescence emission, and anisotropy, we performed a systematic linkage analysis of the three-ligand interaction between MgADP, Fru-6-P, and MgATP. We found that MgADP at low concentrations did not enhance or inhibit substrate binding. Anisotropy shows that MgADP binding at the allosteric site occurred even when MgADP produced no allosteric effect. However, as in the wild-type enzyme, the binding of MgADP to the active site in the mutant competitively inhibited MgATP binding and noncompetitively inhibited Fru-6-P binding. These results clarified the mechanism of a three-ligand interaction and offered a nontraditional perspective on allosteric mechanism.

A notable feature of MgADP as an allosteric effector of *Escherichia coli* phosphofructokinase (PFK)[1] is the apparent paradoxical dual role MgADP plays toward the enzyme. The enzyme's affinity for fructose 6-phosphate (Fru-6-P) increases when MgADP binds to the allosteric site, but the affinity for Fru-6-P decreases when MgADP binds to the active site (*1*−*3*). MgADP activates Fru-6-P binding by approximately 6-fold (unpublished observation) but inhibits binding by 60-fold (*1*). Since linkage imposes a mutually reciprocal binding effect, the enzyme's affinity for MgADP is altered by the same magnitude—whether Fru-6-P binds to the enzyme prior to or after MgADP binding. When Fru-6-P is absent, MgADP binds to each site with equal affinity ($[K_x] = 13\ \mu M$).

Crystallographic data on the wild-type PFK revealed that MgADP interacts with the active and allosteric sites primarily through its phosphate groups, leaving the surface of the nonparticipating adenine slightly exposed to solvent. In the allosteric site, the octahedrally coordinated Mg^{2+} ion bridges the α- and β-phosphates of ADP to the carbonyl oxygen of glycine (Gly) 185 and to the carboxylate of glutamate (Glu) 187 (*4*). This three-way interaction is inferred to be the principal mechanism of allosteric action. Indeed, certain reports have advanced a theory that Glu 187 may be the "trigger" residue for allosteric responsiveness in *E. coli* PFK (*5*−*7*). Numerous site-specific mutations of Glu 187 relating to packing properties and charge attributions were altered

† This work was performed at Texas A&M University in partial fulfillment of the dissertation for the Ph.D. in Biochemistry and was supported by Grant GM-33216 from the National Institutes of Health.

* To whom correspondence should be addressed at the Division of Pathology and Laboratory Medicine, The University of Texas M. D. Anderson Cancer Center, 1515 Holcombe Blvd., Box 84, Houston, TX 77030. Phone: 713-792-0729. Fax: 713-792-0936. E-mail: aspham@mail.mdanderson.org.

‡ The University of Texas M. D. Anderson Cancer Center.

§ University of Oklahoma.

|| Texas A&M University.

[1] Abbreviations: PFK, phosphofructokinase; Fru-6-P, fructose 6-phosphate; Gly, glycine; Glu, glutamate; Ala, alanine; PEP, phosphoenolpyruvate; LB, Luria broth; EPPS, *N*-(2-hydroxyethyl)piperazine-*N*′-3-propanesulfonic acid; EDTA, ethylenediaminetetraacetic acid; NADH, nicotinamide adenine dinucleotide; MOPS, 3-(*N*-morpholino)-propanesulfonic acid; V_{max}, maximum saturation. *K* generally describes an equilibrium value; in accordance with Cleland's convention in which A, B, and C represent substrates and X, Y, and Z represent effector ligands, we represent subscripts a = Fru-6-P, b = MgATP, x = MgADP, and y = PEP such that K_a (or $K_{1/2}$) is the substrate concentration at half-maximal rate (under certain conditions of rapid equilibrium and steady-state conditions, $K_{ia} = K_a$), K_{ia} is the dissociation constant for Fru-6-P, and $K_{a/y}$ is the dissociation constant for Fru-6-P under saturating PEP concentrations). *Q* generally describes a coupling constant (e.g., $Q_{ax/y}$, coupling constant for Fru-6-P and PEP in saturating MgATP; Q_{ax2}, coupling constant for Fru-6-P and MgADP when MgADP is bound at the active site).

10.1021/bi001768z CCC: $20.00
Published on Web 03/07/2001

in these studies (*5*−*7*). These mutations commonly resulted in reduced catalytic turnover activities or decreased binding affinities. The most notable of these mutations is the Glu 187-to-alanine (Ala) modification, whereby phosphoenolpyruvate (PEP) enhances Fru-6-P binding and MgGDP loses its allosteric responsiveness (*5*, *6*). In the wild-type enzyme, MgGDP also activates Fru-6-P binding (*1*, *2*, *5*, *8*−*10*). Since allosteric effects are inferred from ligand binding and commonly detected by enzymatic assays, Lau and Fersht have at first surmised that MgGDP does not bind to the E187A mutant PFK enzyme (*6*). Subsequently, by carrying their enzymatic kinetic assays out to higher MgGDP concentrations, they concluded that MgGDP binds to the allosteric site and reverses from activation to inhibition. The reported inhibition constant for MgGDP is an unusually high K_i of approximately 11 mM (*5*). MgGDP presumably interacts with residue 187 to induce a quaternary conformational switch or stabilize the inactive (T) conformation of the mutant enzyme (*11*). Conversely, in the wild-type enzyme, MgGDP presumably promotes the R state and PEP promotes the T state. These results are seemingly consistent with the predictions of the classical two-state allosteric theory (*7*).

In this report, we propose an alternative explanation to the above conclusion. There appears to be a well-known but underreported controversy pertaining to the role MgGDP plays toward *E. coli* PFK. Some researchers prefer to use MgGDP, rather than MgADP, because MgGDP is *presumed* not to bind to the active site and thus is *presumed* to prevent certain experimental complications (*1*, *2*, *5*, *8*−*10*). After reviewing past publications to assess the role of MgGDP in PFK, however, we cannot conclude that MgGDP binds exclusively to the allosteric site (*2*, *8*, *12*, *13*). The first of these reports came from a classic, well-cited PFK work, from which described the authors' examination of possible interactions of several nucleotide diphosphates and triphosphates with binding sites and their roles in catalysis (*2*). Blangy et al. showed that triphosphates *other* than MgATP can serve as phosphoryl donors, even though their binding affinities are comparatively lower (*2*). It follows that the active site binding pocket will probably accommodate, among others, MgGDP as the byproduct of a catalyzed reaction from which MgGTP served as the substrate. Similar to the action by MgADP, MgGDP binding to the active site perhaps also antagonizes Fru-6-P binding through charge repulsion of the phosphate groups. Brynes et al. (*12*) have shown for *Bacillus stearothermophilus* PFK that MgGDP activates at low, but inhibits at high, MgGDP concentrations. Furthermore, the authors distinguished the inhibition by MgGDP at high concentrations to be noncompetitive toward Fru-6-P and competitive toward MgATP (*12*). While the dual activation/inhibition actions of MgGDP have not been demonstrated conclusively for *E. coli* PFK, because of an inherent binding affinity problem, qualitatively comparable results have been reported for MgADP (*1*). Also, MgGDP has been shown to enhance Fru-6-P binding by a magnitude equivalent to MgADP, that is, a 6-fold activation in *E. coli* PFK (*8*, *13*). While we do not attempt to equate quantitatively the actions of MgGDP and MgADP, the only significant difference we noted between MgGDP and MgADP is the affinity of each toward the binding sites. MgADP appears to bind to the allosteric site with a 5-fold higher affinity than MgGDP (*6*). Thus, the inhibition at extremely high MgGDP concentrations in the E187A mutant reported by other researchers (*6*, *11*) may be due to the competition of MgGDP with the cosubstrate MgATP for binding to the active site rather than to MgGDP binding at the allosteric site. Therefore, it remains inconclusive whether MgGDP and MgADP bind to the regulatory site and what allosteric roles these nucleotide diphosphates play in the *E. coli* E187A mutant PFK.

The unique tryptophan (Trp 311) per homologous subunit of *E. coli* PFK is a convenient intrinsic fluorescent probe because of its varying degrees of responsiveness toward ligands (*1*, *12*, *14*, *15*). We will show in this report that the modification of Glu 187 to Ala resulted in significant differential steady-state fluorescence changes attributable to ligands binding to the allosteric site. From these distinct changes, we were able to distinguish between ligand-binding events and allosteric phenomena. We report here that MgADP bound to the active and allosteric sites of the E187A mutant with affinities comparable to its binding to the wild-type enzyme, that high concentrations of MgADP noncompetitively inhibited Fru-6-P but competitively inhibited MgATP, and that low concentrations of MgADP competitively inhibited PEP but did not affect Fru-6-P binding. Furthermore, both the magnesium (or other divalent metals) and the nucleotide diphosphate contributed to the allosteric effects, rather than the nucleotide diphosphate alone.

EXPERIMENTAL PROCEDURES

Materials. All reagents used in buffers and in PFK purification, enzyme kinetics, and fluorescence studies were of analytical grade and were purchased from either Sigma (St. Louis, MO) or Fisher Scientific (Pittsburgh, PA). Fru-6-P (disodium salt), ADP (potassium salt), ATP (disodium salt), and PEP (trisodium salt) were obtained from Sigma. Auxiliary enzymes aldolase, triose-phosphate isomerase, and glycerol-3-phosphate dehydrogenase (ammonium sulfate suspensions) were purchased from Roche Diagnostics Corp. (Indianapolis, IN). The pALTER-1 Sites Mutagenesis kit was obtained from Promega (Madison, WI). Matrix Gel Blue A−agarose chromatography resin was obtained from Amicon (Beverly, MA). All buffers and stock ligand concentrations were filtered through a 0.22-μm membrane obtained from Millipore (Bedford, MA).

Site-Directed Mutagenesis and Expression of the pfk-1 Gene. The plasmid encoding the wild-type *E. coli* PFK, pRZ3 (*16*), was a generous gift from Dr. Robert Kemp, as was the host *E. coli* strain DF1020 [*pro*82, Δ*pfkB*201, *recA*56, Δ(*rha-pfkA*), *endA*1, *hsdR*17, *supE*44], from which the *pfk-1* and *pfk-2* genes were deleted (*17*). The *pfk* gene was removed from pRZ3 by digestion with *Bam*H1 and *Hin*dIII restriction enzymes and then introduced into the polyclonal region of the pALTER-1 vector (Promega), yielding pGDR16. Mutagenesis subsequently was performed on pGDR16 using a method prescribed by Promega. The residue Glu 187 was replaced by Ala through a single nucleotide substitution using the primer 5′-CAA-CGA-ATG-CAC-AGC-CAC-3′. The resultant recombinant expression vector, pGDR24, was transformed into the DF1020 host strain using the calcium chloride method (*18*). Sequencing of the entire gene was performed to identify the targeted mutation and affirm that no spurious mutations were created. A single colony was picked, grown in Luria broth (LB), and stored at −80 °C in

10% glycerol. All experiments were performed using the proteins purified from this single LB−glycerol stock. Five milliliter cultures were routinely grown from this LB−glycerol stock for 18−20 h at 37 °C in the presence of 100 μg/mL ampicillin. One milliliter of this culture was then transferred to 2 L of ampicillin-laced LB and grown at 37 °C for no more than 22 h. The culture was harvested by centrifugation at low speed (2000*g*). Two to four liters of culture was routinely grown, yielding approximately 6 g of cells per liter.

Purification of PFK. The purification protocol was modified from the method originally described by Kotlarz and Buc (*19*). *E. coli* cells were lysed using the French press method and then centrifuged at 12000*g* for 1 h. The resulting yellow-colored supernatant was subjected to a 10-min incubation at 37 °C with a trace amount of deoxyribonuclease I and then passed over a resin Matrix Blue A (Amicon) affinity column (~10 mg of protein/mL of resin) at 15 mL/h. The column was washed with Tris-HCl buffer (pH 7.5) until a clear color was obtained. The column was then washed with Tris-HCl buffer containing 1.5 M NaCl until an absorbance of <0.2 unit at 280 nm was reached. The protein was eluted in Tris-HCl buffer containing 1.5 M NaCl, 2 mM ATP, and 20 mM $MgCl_2$. After an extensive dialysis, the protein was then passed through a fast protein liquid chromatography (FPLC) Mono Q HR10/10 anion-exchange column (Pharmacia Biotech, Piscataway, NJ) as a final purification and concentration step. The final eluate was pooled from a continuous 0−1 M NaCl gradient in Tris buffer, dialyzed extensively, and stored in 50 mM *N*-(2-hydroxyethyl)piperazine-*N*′-3-propanesulfonic acid (EPPS)−KOH buffer (pH 8) containing 0.1 mM EDTA. Apparent purity was determined by absorbance readings at 278 nm ($\xi_{278} = 0.6$ cm^2 mg^{-1}) (*19*). To ensure negligible nucleotide contamination, only PFK preparations in which the 280/260 absorption ratio was above 1.8 were used in experiments. The protein yields were approximately 20 mg/L of cells, with specific activities of ~500 and ~300 units/mg for the wild-type and the E187A mutant, respectively.

Enzyme Activity Measurements. Kinetics assays were performed in 50 mM EPPS−KOH buffer (pH 8, 25 °C), 100 mM KCl, 20 mM $MgCl_2$, 2 mM dithiothreitol, 0.1 mM EDTA, and 0.2 mM nicotinamide adenine dinucleotide (NADH). Activity rates were followed by monitoring the oxidation of NADH at 340 nm coupled to the formation of fructose 1,6-bisphosphate by use of the auxiliary enzymes aldolase (250 μg), triose-phosphate isomerase (5 μg), and glycerol-3-phosphate dehydrogenase (50 μg). The auxiliary enzymes were dialyzed extensively and stored in 50 mM 3-(*N*-morpholino)propanesulfonic acid (MOPS)−KOH (pH 7), 100 mM KCl, 5 mM $MgCl_2$, and 0.1 mM EDTA. Stock solutions of Fru-6-P, ADP, ATP, and PEP were diluted appropriately using the same buffer components and brought to the desired pH at the temperature required by experimental specifications. For kinetic experiments in which MgATP was not a dependent variable, a saturating amount of 3 mM MgATP was used. The progress of each reaction was recorded on a strip-chart recorder connected to a Beckman DU spectrophotometer updated with Gilford electronics. Each activity rate was calculated by measuring the slope of a line tangent to the reaction progress curve on centimeter-gauged strip-chart paper (Honeywell, Morristown, NJ), given the extinction coefficient for NADH to be 6.22×10^3 M^{-1} cm^{-1}. No pre-steady-state bursts or lags were observed under the conditions described. Substrate concentration depletion was less than 5%, since the reaction never proceeds to a significant extent. Thus, the amount of MgADP produced from the catalyzed reaction did not interfere with the amount of MgADP added as the independent variable. The concentration of Fru-6-P required to give the half-maximal rate, $K_{1/2}$, was determined from the Hill equation (*20*) at a certain effector concentration. In most cases, a series of $K_{1/2}$ values are determined in the presence of another ligand at different fixed concentrations.

Steady-State Intensity Emission Measurements. Fluorescence intensity measurements were determined using an SLM 4800 fluorometer modified with ISS photon-counting electronics (PX01) and operating software. A xenon arc lamp was the source of excitation, and the monochromator grating provided a source of wavelength selection. Intensity measurements were obtained either by scanning the emission range of 310−475 nm or by integrating the emission at 350 nm for 10 s. The intensities were adjusted with neutral density filters (Corning) placed in the path of the excitation beam to provide a counting rate of <100 kHz. To prevent the appearance of an artifactual hump in the 400-nm region due to a grating imperfection, a vertically oriented polarizer was placed in the emission pathway when collecting emission spectra. The intrinsic tryptophanyl fluorophore was excited at 300 nm to avoid concurrent excitation of tyrosine residues and to minimize the inner filter effect due to high concentrations of nucleotides. Buffer components were the same as specified for the kinetics experiments. For the metal-binding experiments, the EDTA concentration was reduced to 10 μM. Measurements were performed by titrating the substrate and/or allosteric ligand into a 1 × 1 cm cuvette (Helma) containing 0.5 μM (0.02 μg/μL) PFK subunit concentration in a 2-mL volume. The protein concentration used was at least 10-fold below the ligand concentration at half-maximal saturation to ensure that the concentration of the free ligand approximated that of the total ligand. Buffer blanks were subtracted to correct for H_2O Raman scattering and background fluorescence due to contaminants in the buffer components. Emission intensity was corrected for volume changes associated with ligand additions, and the data were normalized with respect to the initial baseline value of 1.

Steady-State Anisotropy Measurements. Each anisotropy value was determined from a blank-subtracted sample, where the blank cuvette contained all components except for the protein containing fluorophore

$$\frac{I_{\parallel}}{I_{\perp}} = \frac{(I_{VV(sam)} - I_{VV(blk)})(I_{HH(sam)} - I_{HH(blk)})}{(I_{VH(sam)} - I_{VH(blk)})(I_{HV(sam)} - I_{HV(blk)})} \quad (1)$$

where the subscript letter immediately following *I* indicates the position of the excitation polarizer and the second subscript indicates the position of the emission polarizer. V and H designate vertical and horizontal, respectively. The *G* factor, a normalization value used to correct for an instrumental defect that caused $I_{\parallel}$ to be not precisely equal to $I_{\perp}$ when a sample is completely depolarized (*21*), was determined by recording the ratio of vertical and horizontal emission intensities with the excitation polarizer oriented horizontally. This I_{HV}/I_{HH} ratio is incorporated into eq 1.

Anisotropy values were calculated from the expression:

$$r = \frac{(I_{\parallel}/I_{\perp}) - 1}{(I_{\parallel}/I_{\perp}) + 2} \quad (2)$$

A Schott WG-345 filter was placed between the sample and the photomultiplier tube to allow emission intensities beyond 345 nm to be measured. Each final data point represents an average of two or three sets of measured anisotropy values, with each set consisting of an average of 8−12 measurements.

Atomic Absorption Spectroscopy. Metal contaminants were removed from the protein by incubation with 20 mM EDTA overnight; the protein was then extensively dialyzed in 50 mM metal-free EPPS−KOH (pH 8, 25 °C) buffer with 10 μM EDTA. The Mg^{2+} content of PFK was determined using a Perkin-Elmer 2380 atomic absorption spectrometer operating in the furnace mode. Detection was monitored at 285.2 nm (slit 0.7 nm) using a magnesium hollow-cathode lamp (Photonics K.K) operating at 18 mA. A standard curve for magnesium was generated using a concentration range of 0−2 μM.

Data Analysis. For kinetic analyses, we assumed a rapid equilibrium condition in which the enzyme or substrate achieved an approximate binding equilibrium in a steady state (*14*, *22*, *23*). Data were fit to the Hill equation, allowing the Hill number, V_{max}, and $K_{1/2}$ to float:

$$v = \frac{V_{max}[A]^{n_H}}{K_{1/2}^{n_H} + [A]^{n_H}} \quad (3)$$

Each fluorescence titration profile was fit to the expression accounting for a nonzero baseline:

$$\Delta F = \frac{\Delta F_{\infty}[X] + F_0(K_d) + F_0[X]}{K_d + [X]} \quad (4)$$

where ΔF represents the apparent fluorescence change, ΔF_{∞} denotes the maximal fluorescence change when X is present in a saturating amount, and F_0 is the initial fluorescence value (generally normalized to 1).

The variation of the apparent $K_{1/2}$ for Fru-6-P was determined as a function of fixed concentrations of allosteric ligand ([X]). The $K_{1/2}$ or K_d values, obtained from either eq 3 or eq 4 as a function of a second ligand, were then fit to the linkage expression (*24*−*26*):

$$K_{1/2} = K_{ia}^{\circ}\left(\frac{K_{ix}^{\circ} + [X]}{K_{ix}^{\circ} + Q_{ax}[X]}\right) \quad (5)$$

where $K_{1/2}$ (or K_a) represents the apparent dissociation constant for the substrate, K_{ix}° represents the dissociation constant for the allosteric ligand, X, in the absence of substrate, and Q_{ax} is the coupling limit describing the nature and magnitude of the allosteric effect. Q_{ax} is equal to the ratio of $K_{ia}^{\circ}/K_{ia}^{\infty}$, where K_{ia}° corresponds to the substrate dissociation constant at zero allosteric ligand concentration and K_{ia}^{∞} corresponds to the plateau value approached at high allosteric ligand concentrations. Equations were fit using nonlinear regression programs written either in the C programming language and run on a Silicon Graphics Personal Iris workstation or in Kaleidagraph (Synergy Software) and run on a 7100 Power PC Macintosh.

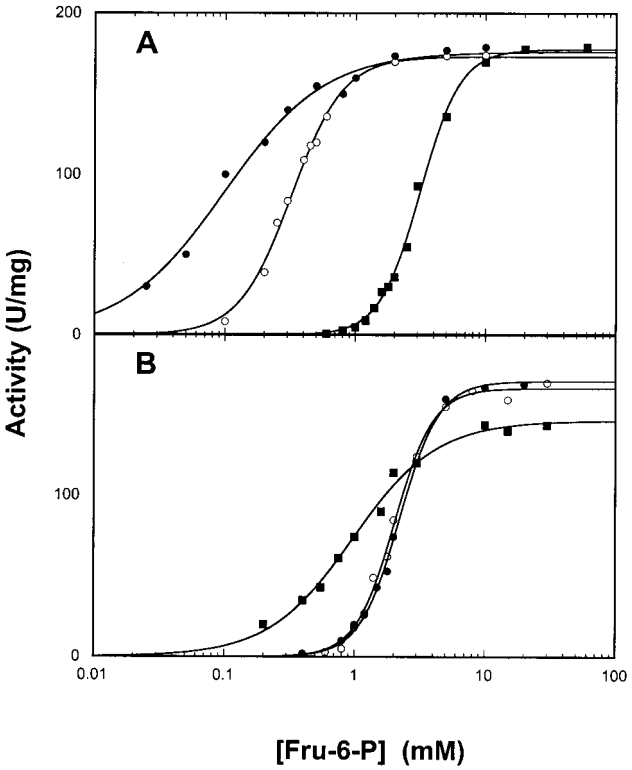

FIGURE 1: Dependence of allosteric ligands on the Fru-6-P isothermal activity profile for the wild-type (A) and the E187A mutant (B) PFK. Activities were determined in no effector ligand (○), 0.5 mM MgADP (●), or 2 mM PEP (■). The solid lines represent the fits to the Hill equation to obtain $K_{1/2}$ values.

RESULTS

Effect of the E187A Mutation on the Enzyme's Affinity for Fru-6-P. Since most experiments for the wild-type enzyme were performed previously using 20 mM NH_4Cl (*1*, *3*, *14*, *15*), it was necessary to assess the salt conditions for possible quantitative comparisons between the wild-type and the E187A mutant enzymes. These experiments were also designed to address a discrepancy, a 4-fold difference in the affinity of Fru-6-P, between our findings and those reported by other authors (*6*). Enzymatic assays were performed as described in the Experimental Procedures section with the exception that the monovalent salt used was either 20 mM NH_4Cl or 100 mM KCl. We found no significant differences in binding between the two salt concentrations for the wild-type enzyme ($K_{1/2}$ ~0.3 mM), but the E187A mutant showed a modest, yet noteworthy, decrease in binding affinity at the higher salt concentration. The E187A mutant exhibited $K_{1/2}$ values of 1.8 ± 0.2 mM in 100 mM KCl and 0.5 ± 0.03 mM in 20 mM NH_4Cl. The latter result is similar to that reported by Lau and Fersht, but they did not report the monovalent salt concentration (*5*, *6*). Thus, the salt concentration may account for the differences in the dissociation constants between those reported here and those reported by Lau and Fersht. The salt-dependent $K_{1/2}$ that was displayed by the E187A mutant mimics the *K*-type activation by NH_4Cl observed in mammalian PFK (*27*, *28*). In either case, the difference in substrate binding affinity was small, and no other notable differences were observed under these

salt conditions. Since 100 mM KCl closely resembles the physiological environment of a cell, this salt concentration was used in all subsequent experiments.

Mutational Effects on Fluorescence Properties for Ligand Binding. The apparent steady-state fluorescence emission intensities for substrates binding to the active site of the E187A mutant were similar to those of the wild-type enzyme, in that Fru-6-P produced a 30% reduction and MgATP a 13% increase in the emission intensity (data not shown). In contrast, effector ligands binding to the allosteric site showed dramatic changes. No fluorescence change was observed upon addition of up to 2 mM MgADP or 60 mM PEP to the E187A mutant. The same MgADP and PEP concentrations caused a 28% reduction and a 9% increase, respectively, in emission intensities for the wild-type PFK enzyme.

Under identical experimental conditions, anisotropy values for the uncomplexed enzyme form were 0.204 for the wild type and 0.194 for the mutant. This minor discrepancy in anisotropy values may be attributed to the mutation, since increasing the PFK subunit concentration of the E187A mutant increased the anisotropy value to 0.203 (discussed below). Substrate binding to the wild-type and the E187A mutant PFKs produced comparable results, a 0.02 decrease in the saturating amount of Fru-6-P and a 0.01 increase in MgATP. Anisotropy changes for ligands binding to the allosteric site of the mutant were considerably different from those of the wild-type enzyme. A marginal anisotropy increase was observed for MgADP (0.005) while a substantial decrease (0.03) was observed for PEP in the wild-type enzyme. In contrast, no anisotropy change is detected from the addition of up to saturating amount of PEP but a significant 0.02 increase in anisotropy value upon the addition of 0.5 mM MgADP. Additional MgADP of up to 1 mM further augments anisotropy to a final value of 0.221.

Loss of Allosteric Effect by MgADP on the E187A Mutant PFK. While the E187A mutation modestly affected ligand binding to the free enzyme complex, the impact of the mutation was most evident when binding occurred in the presence of other ligands. Figure 1 compares the influence of allosteric ligands on the isothermal activity profiles between the wild-type and the mutant enzymes. For the wild-type enzyme, the substrate concentration producing half the maximal rate was shifted left or right in response to an activator or inhibitor, respectively, with no change in the maximal turnover rate (Figure 1A). In contrast, introduction of the inhibitor PEP to the E187A mutant weakly activated the binding affinity and inhibited the V_{max} (Figure 1B). MgADP appeared to be having no effect on the binding of Fru-6-P since the binding profiles of Fru-6-P in the presence and absence of MgADP were nearly superimposed.

Figure 2 compares the dependence of $K_{1/2}$ values for Fru-6-P on MgADP for the wild-type and E187A mutant enzymes. MgADP enhanced the binding affinity of the wild-type enzyme for Fru-6-P, indicated by the decreasing $K_{1/2}$ when the MgADP concentration increased from 0 to 8 mM. Fit of the data to eq 5 indicated that the magnitude of this *K*-type activation was approximately 6-fold ($Q_{ax} = 6.4 \pm 0.3$). The E187A mutant, however, exhibited an unchanged $K_{1/2}$ for Fru-6-P binding at all MgADP concentrations up to 8 mM. The coupling Q_{ax} value was 1.1 ± 0.1, indicating no allosteric effects.

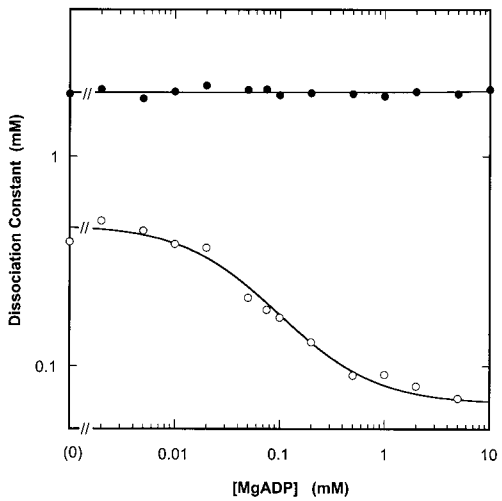

FIGURE 2: Effect of MgADP on the apparent dissociation constant for Fru-6-P for the wild-type (○) and the E187A mutant (●) PFK. $K_{1/2}$ for Fru-6-P was determined by varying MgADP concentrations from 0 to 5 mM while keeping the MgATP concentration at least 2-fold higher than that of MgADP.

Our results are consistent with previous reports showing that the allosteric effect by MgADP is abolished in the mutated E187A (*6*, *7*). These reports were based primarily on enzymatic activity assays, and the ligand-binding measurements were performed in the presence of some saturating amount of MgATP to drive the reaction forward. Other works have shown that MgATP modifies the extent of the coupling interactions between Fru-6-P and its allosteric effectors (*1*, *3*, *25*). MgATP has been shown to decrease the enzyme's affinity for Fru-6-P by ~10-fold (*1*, *3*). Thus, MgATP may play a significant role in abolishing this allosteric influence by MgADP. To determine whether the abolishment of this allosteric influence by MgADP toward Fru-6P prevails when MgATP is absent, we monitored the fluorescence emission produced by the coupling of Fru-6-P and MgADP. Fluorescence change was recorded at each titration of Fru-6-P into a cuvette containing the enzyme and a particular fixed concentration of MgADP. The experiment was repeated until a two-dimensional array was formed in series of MgADP and Fru-6-P concentrations. Figure 3 shows the relative quenching amplitudes of the steady-state fluorescence emission for Fru-6-P at various fixed concentrations of MgADP. In the wild-type enzyme, quenching of Fru-6-P was maximal when MgADP was absent. Increasing MgADP dramatically dampened the amplitude, as evidenced by the flattening of the curves (Figure 3A). Fru-6-P and MgADP each caused an approximate 30% quenching of fluorescence emission intensity, but together they produced only ~11% quenching.

The Fru-6-P/MgADP interaction in the E187A mutant displayed a pattern of intensity changes very different from that in the wild-type enzyme. Titration of Fru-6-P to the E187A mutant in the presence of low MgADP concentrations augmented the amplitude of quenching by ~10%. MgADP at a concentration of 10 μM contributed Fru-6-P quenching to a total of 40% reduction in the emission intensity. Recall that the addition of MgADP alone to the *E. coli* E187A mutant PFK did not produce emission intensity changes. The concentration of MgADP that produced the most drastic change was ~10 μM; its significance is discussed below. No further quenching was observed at MgADP concentrations higher than 10 μM.

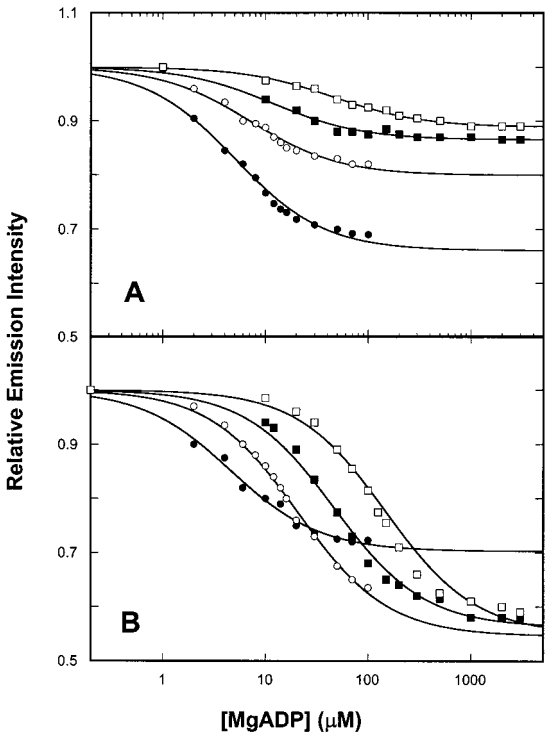

FIGURE 3: Relative quenching amplitude of the fluorescence emission intensity changes upon the addition of Fru-6-P in the presence of 0 (●), 0.01 mM (○), 0.1 mM (■), and 1 mM (□) MgADP for the wild-type (A) and the E187A mutant (B) PFK. Each binding profile was fit eq 4 to obtain the dissociation constant for binding.

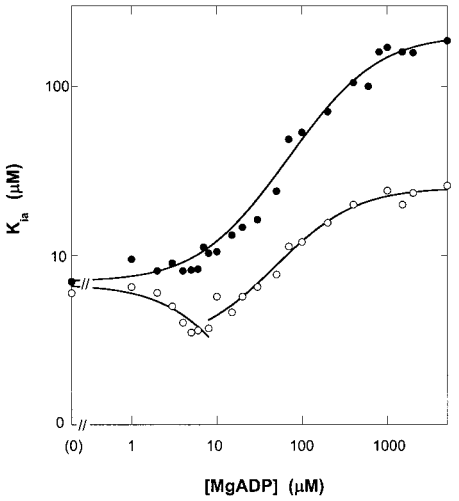

FIGURE 4: Dependence of the dissociation constant for Fru-6-P as a function of MgADP for the wild-type (○) and the E187A mutant (●) PFK. Each K_{ia} value was determined from the fit of the fluorescence emission fractional saturation profile to eq 4. The solid lines represent the fit of the data to eq 5 (where $K_{1/2}$ is considered equivalent to K_a) to yield K_{ia}, K_{ix}, and Q_{ax}.

Inhibition of Fru-6-P by MgADP Binding to the Active Site of the E187A Mutant PFK. Figure 4 compares the dependence of the dissociation constant (K_{ia}) for Fru-6-P as a function of MgADP, determined from fluorescence emission intensity, for Fru-6-P of the wild-type and the mutant enzymes. The wild-type enzyme displayed a biphasic pattern in which Fru-6-P binding affinities were enhanced at low MgADP concentrations (indicated by the decreasing K_{ia} values) but was impeded at higher MgADP concentrations (indicated by the increasing K_{ia} values). In contrast, the K_{ia} trend for the E187A mutant displayed a single phase, from which the segment of decreasing values in the low MgADP range was absent. The sharp monophasic increase in the dissociation constant indicates that MgADP exerted a powerful inhibitory effect on the mutant enzyme's affinity for Fru-6-P. This inhibition was presumably due to the negatively charged repulsion between the phosphate groups of Fru-6-P and MgADP, which occurs when MgADP binds to the *active* site. The inhibitory effect of MgADP on the binding of Fru-6-P was not observed in enzymatic catalysis when MgATP was present in a saturating amount. MgADP binds at a much lowered affinity than MgATP and, therefore, requires a higher amount to overcome MgATP's binding, resulting in a higher dissociation constant. The results reported here may explain Lau and Fersht's finding of a dissociation constant for MgGDP of ~11 mM in the E187A mutant. A concentration of 1 mM MgATP was used in those experiments (*5*, *6*). The data suggest that the fluorescence emission changes for the E187A mutant are due to MgADP binding to the *active* site.

Table 1: Dissociation Constants for Fru-6-P or MgADP in the E187A Enzyme

ligand	other saturating ligand	designation	dissociation constant (mM)
Fru-6-P		K°_{ia}	0.009 ± 0.001
Fru-6-P	MgATP	$K^{\circ}_{ia/b}$	1.8 ± 0.2
Fru-6-P	$MgADP_{(eff)}$[a]	$K^{\circ}_{ia/x1}$	0.005 ± 0.001
Fru-6-P	$MgADP_{(act)}$[a]	$K^{\circ}_{ia/x2}$	0.21 ± 0.06
Fru-6-P	$MgADP_{(eff)}$, MgATP	$K^{\circ}_{ia/bx1}$	2.2 ± 0.03
$MgADP_{(eff)}$		K°_{ix}	0.008 ± 0.0001
$MgADP_{(eff)}$	PEP	$K^{\circ}_{ix/y}$	0.026 ± 0.003
$MgADP_{(eff)}$	Fru-6-P, MgATP	$K^{\circ}_{ix/ab}$	0.007 ± 0.001
$MgADP_{(act)}$		K°_{ix2}	0.29 ± 0.02
$MgADP_{(act)}$	Fru-6-P	$K^{\circ}_{ix2/a}$	0.25 ± 0.02

[a] $MgADP_{(eff)}$ = MgADP binding to the allosteric site; $MgADP_{(act)}$ = MgADP binding to the active site.

To confirm that MgADP also binds to the active site of the E187A mutant with an affinity indistinguishable from which it binds to the wild-type counterpart and that MgADP competitively inhibits MgATP, we determined the Michaelis−Menton constants for MgATP at fixed concentrations of MgADP. The reaction mixture included Fru-6-P kept at a saturating concentration of 10 mM, well in excess of its dissociation constant. Data were fit to eq 3 (setting n_H to 1) by using both the nonlinear regression and the linear double-reciprocal forms. Since MgATP did not appear to display any form of homotropic or heterotropic cooperativity, double-reciprocal plotting was possible. The V_{max} values converged to a single point on the *y*-intercept, indicating that the inhibition of MgATP by MgADP was competitive. Fitting the binding profiles for each concentration of MgADP to the Michaelis−Menton equation via nonlinear regression analysis yielded similar results for the invariant V_{max} and linearly dependent K_m values. The K_{ix} was determined from the slope to be 290 ± 20 μM, a value that is indistinguishable from that of the wild-type enzyme.

Table 1 summarizes the dissociation constants for Fru-6-P and MgADP in the absence and presence of saturating amounts of other ligands. In general, the dissociation constants for each ligand binding to the enzyme in the absence of other ligands are indistinguishable from those

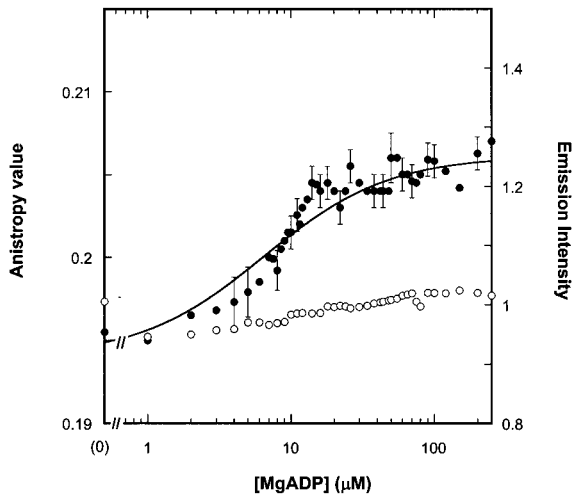

FIGURE 5: Modification of the steady-state anisotropy value (●) upon the addition of MgADP to the E187A mutant PFK. The solid line represents the fit of the data to eq 4 (K_{ix} = 8.2 ± 0.7 μM). The emission intensity (○) remains relatively constant for up to 0.25 mM MgADP.

found in the wild-type enzyme. Altering the Glu at position 187 to an Ala did not affect the binding affinity of either Fru-6-P or MgADP. Dissociation constant differences between the wild-type and the E187A mutant enzymes are most striking when a second or third ligand is present. For example, when MgATP was present, the dissociation constant for Fru-6-P was 1.8 mM (~0.3 mM for the wild-type enzyme); when both MgADP and MgATP were present, the dissociation constant for Fru-6-P was 2.2 mM (~0.05 mM for the wild-type enzyme).

MgADP Binding to the Allosteric Site of the E187A Mutant. Evidence for the interaction of MgADP with the allosteric site is derived from fluorescence anisotropy measurements and is shown in Figure 5. Adding up to 50 μM of MgADP to the E187A mutant resulted in an increase in the anisotropy value from 0.195 to 0.207. Although the change was small, there is a pattern of consistent augmentation in anisotropy values that is associated with increasing MgADP concentrations and is characteristic of an isothermal binding profile. Figure 5 also shows that the fluorescence emission intensity, derived simultaneously with the anisotropy measurements, remained relatively constant throughout the range of MgADP concentrations examined. Fit of the anisotropy data to eq 5 yielded a K_{ix} of 8.2 ± 0.7 μM. Other experimental data suggest that this value reflects the dissociation constant of MgADP binding to the allosteric site. We previously described the intensity emission changes for Fru-6-P when MgADP is present, presumably in the binary enzyme complex form. The intensity emission change for Fru-6-P appeared to be most dramatic at a MgADP concentration of ~10 μM, suggesting the dissociation constant for MgADP to be ~10 μM when MgATP is absent. Figure 3B also shows that Fru-6-P quenching occurred most drastically at 10 μM MgADP. Indeed, a ligand usually exerts its most potent effects and produces maximum changes in fractional binding at concentrations within the range of its dissociation constant.

To ascertain whether MgADP caused the observed fluorescence phenomena, we considered the possibilities of artifacts or nonspecific interactions that could have caused the fluorescence responses. First, it is conceivable that the observed anisotropy changes were due to the product of MgADP hydrolysis upon storage since stock concentrations of the ligand were prepared for multiple measurements to reduce experimental errors. Over time, MgADP perhaps breaks down to MgAMP + P_i, and the changes observed may have been due to MgAMP rather than MgADP. To test this possibility, fluorescence intensity and anisotropy properties were determined for the E187A mutant PFK protein in the presence of 200 μM MgAMP. As was the case for MgADP, MgAMP apparently caused no changes in the emission intensity. However, in contrast to the increasing anisotropy values for MgADP (shown in Figure 5) MgAMP produced a distinct 0.013 *decrease* (from 0.195 to 0.182) in the anisotropy value. Second, contamination of adenylate kinase may be possible, but the emission intensity changes attributed to the binding of MgATP were inconsistent with those observed for MgADP. The 13% increase of emission intensity observed for MgATP was not observed with increasing MgADP concentrations (Figure 5); thus, fluorescence changes could not be due to contamination by MgATP. Third, anisotropy changes may reflect changes in the oligomerization states of the protein rather than MgADP binding. We have noted that the anisotropy values in the presence of MgADP were different in the two enzyme types. However, the differences in the anisotropy values were apparently not dependent on time and, therefore, cannot reflect transitions in the protein subunits as reported for the oligomerization phenomena in mammalian systems (*29*−*31*). Systematic experimental analyses are needed to examine this possibility.

Mutually Exclusive Interaction of MgADP with PEP. Using steady-state anisotropy, we measured the apparent dissociation constant for MgADP at each constant PEP concentration. Each resultant binding profile was fit to eq 4. Plotting the K_{ix} for MgADP as a function of PEP concentration yielded a directly proportional relationship that is indicative of competitive binding between MgADP and PEP. Crystallographic data indicate that both allosteric effectors bind to the same allosteric site while the occupation of the active site by MgADP hardly hinders PEP binding (*4*, *32*). The mutually exclusive relationship between MgADP and PEP provides convincing evidence that MgADP interacts at the allosteric site. It is this interaction at the allosteric site that had no apparent functional consequence. Results from a complete three-dimensional matrix of ligand interactions between Fru-6-P and PEP in a fixed concentration of MgADP substantiate the results obtained from fluorescence. A fit of the data to eq 5 indicates that systematic increases in MgADP concentration yielded proportionate increases in K_d for PEP. The dissociation constants for Fru-6-P and coupling constants for Fru-6-P−PEP interaction ($Q_{ay/b}$) remained constant (data not shown).

Interaction of a Divalent Metal and ADP at the Allosteric Site. Although it had been shown that magnesium is required for the phosphoryl transfer reaction by PFK (*28*, *33*, *34*), it is uncertain whether a magnesium ion is required for ADP to bind to the allosteric site of the E187A mutant. Since Glu 187 putatively interacts with MgADP through Mg^{2+}, we sought to elucidate the role of Mg^{2+} and other divalent metals. Specifically, is the anisotropy change observed attributable solely to the magnesium ion, to ADP interacting

with the allosteric site, or to MgADP? We addressed this question by monitoring anisotropy changes for the E187A mutant upon addition of magnesium, ADP, magnesium after a short enzyme incubation with ADP, and ADP after an enzyme incubation with magnesium. The binding experiments were performed after an extensive EDTA dialysis and verification by atomic absorption that the magnesium contamination, if any, was negligible. Absorbance measurements of the final dialysate and protein sample indicated that the Mg^{2+} content was <0.2 mol/subunit mol of PFK. Except for reducing the EDTA concentration to 10 μM, all other solution conditions were identical to those used in the previous experiments.

Adding ADP alone produced no changes in the anisotropy values. Likewise, titration of $MgCl_2$ alone did not yield differences in anisotropy values. However, adding one component in the presence of saturating concentrations of the other component produced anisotropy changes that were comparable to those seen with MgADP titration. We also monitored anisotropy changes for the E187A mutant upon addition of other metals with the same coordination number as Mg^{2+}, such as Ca^{2+} and Mn^{2+}. Owing to the high level of noise associated with the sample, we could not ascertain the influence of Ca^{2+}. $MnCl_2$ produced results similar to those of Mg^{2+} and produced no fluorescence changes in anisotropy values. Titration of ADP in 2 mM $MnCl_2$ produced anisotropy increases that were comparable to those obtained upon the addition of ADP into $MgCl_2$ (data not shown). The divalent metal requirement for nucleotide binding to the allosteric site has also been implicated for mammalian PFK (*31*).

DISCUSSION

The results reported here indicated that the binding of MgADP to the E187A mutant of *E. coli* PFK is independent of allosteric responsiveness by MgADP. Other researchers have alluded to this independence relationship through mutation-induced loss of allosteric effects without apparent loss to binding (*7*, *35*). Shortening the side chain of residue 187 by site-specific mutation from a glutamate to an aspartate led to the loss of allosteric influence by PEP while hardly affecting activation by MgGDP (*7*). Binding was inferred from thermal denaturation studies. Removal of approximately 50 C-terminal residues, which affected packing, caused both effector ligands to lose their allosteric effects (*35*). Mutation of an active site residue also abolished inhibition by PEP, even though binding exists (*7*).

For the first time, we were able to quantify the binding affinity of an allosteric ligand even though there was no apparent functional consequence to the enzyme. Evidence for MgADP binding to the allosteric site came from an isothermal saturation profile measured from anisotropy measurements (Figure 5) and enzymatic competition assays (data not shown). Dynamic fluorescence and stopped-flow techniques also provided additional evidence for MgADP binding to the allosteric site (*36*). Furthermore, we have found that linkage between MgADP and Fru-6-P was maintained under preequilibrium conditions (*36*). Our results indicate that Glu 187 participates predominantly in regulation rather than binding. Regulation may be achieved by the repositioning and poising of the MgADP molecule for subunit communication. This repositioning event may occur simultaneously with binding or after binding has occurred, and our data suggest that the binding and reorientation events occurred independently of each other. The reorientation may act as a triggering mechanism to allow communication to occur. Thus, even after the binding event has occurred, the inability to correctly position the ligand molecule may cause ineffectual execution of allosteric communication.

Discerning the role of magnesium may provide insight into the importance of correct positioning of the ADP molecule to the protein. Since anisotropy responses can occur only in the presence of both magnesium and ADP, MgADP rather than ADP alone is necessary for binding. Crystallographic data reported by Shirakihara and Evans (*4*) indicated that the mutation of Glu 187 might affect predominantly the binding of the magnesium ion, leading to incorrect positioning of the ADP. Also, Reinhart and Lardy (*37*) reported that MgATP but not ATP inhibits the activity of mammalian PFK. We have shown that a larger divalent metal with the same coordination number gives a fluorescence signal similar to that of magnesium. Using larger metal ions, which can compensate for the loss of residue packing, might restore the allosteric responsiveness toward Fru-6-P. However, these experiments would be difficult to perform owing to large errors associated with the experimental setup.

Other researchers viewed MgGDP (or MgADP) as an allosteric inhibitor of Fru-6-P binding to the E187A mutant (*6*, *7*). This perspective appeared to be consistent with the classical Monod−Wyman−Changeux (MWC) two-state model (*38*). The MWC model presupposes an enzyme to exist in equilibrium of R (active) and T (inactive) states. According to this model, allosteric inhibitors promote the T state either by inducing a quaternary conformational change to such state or by stabilizing the existing T state of a protein; likewise, the activators induce a change to or promote the R state of a protein. Given that the wild-type inhibitor PEP was found to activate and MgGDP was interpreted by others to inhibit the E187A mutant, it was concluded that residue 187 appears to function as a balance between activation and inhibition (*6*, *7*). Hence, it became a precept that substituting an Ala for this Glu at position 187 causes a switch of the T and R conformations resulting in MgGDP stabilizing the T conformation and PEP stabilizing the R conformation (*11*). Whether this T-to-R switch was caused by a residue change at position 187, mainly affecting the charged−charged interaction between the residue and the nucleotide, or caused by the mutation, affecting the global packing of the enzyme, remains to be distinguished. Lau and Fersht opted for the first explanation, dubbing residue 187 as the "trigger" mechanism (*7*). Because we were able to discriminate ligand binding from allosteric action and to discriminate ligand binding to the allosteric site from ligand binding to the active site, the T-to-R switch theory cannot be sustained regardless of the mechanism at play.

First, a basic assumption of the model is that the uncomplexed form of the enzyme is predominately in the T state. Binding of the substrate causes the T to R transition, putatively evidenced by a sigmodial isothermal profile. If the E187A mutation induces the T-to-R switch so that the initial uncomplexed form of the E187A mutant is in the R state, then substrate binding to the mutant enzyme will exhibit higher binding affinity and a hyperbolic isothermal profile.

However, the evidence indicated otherwise. Both Fru-6-P and MgATP bind to the E187A mutant with affinities and sigmoidal isothermal profiles comparable to those of the wild-type enzyme. Second, if residue 187 were the trigger mechanism responsible for the allosteric responsiveness of the enzyme, then changing the glutamate to alanine would cause MgADP to inhibit and PEP to activate. The evidence presented in this report indicates that MgADP does not inhibit when binding to the allosteric site. The binding characteristics of PEP also does not conform to the two-state model (*39*). PEP becomes a *K*-type activator, where the enzyme presumably adopts an R conformation, and at the very same time becomes a *V*-type inhibitor, where it assumes a T state (*5*, *6*, *39*). Third, the two-state conformational transition approach assumes the existence of an intrinsic link between ligand−protein interaction and global movements of a protein that resulted in either the R or T state. Quaternary structural movement is inferred from changes in steady-state fluorescence intensity emission upon ligand binding and has been equated with the R and T states (*40*). This assumption fails because the binding of MgADP to the E187A mutant PFK does not manifest in global structural movement. Rather, the binding of MgADP was detected by anisotropy, which measures the differential rotational movements of the unique tryptophanyl fluorophore. Anisotropy changes without intensity emission changes most likely resulted from subtle localized protein perturbations rather than global movements. Last, inherent to the MWC and models incorporating static conformational states is the relationship of ligand binding to functional consequences giving rise to each state. The MWC model accounts for activation (giving rise to R states) and inhibition (giving rise to T states) by regulatory ligands but not for binding without the attainment of allosteric effects. The result reported here, the binding of ligand produced no apparent functional role, is in direct contrast with the MWC model.

The data indicate that the inhibition of Fru-6-P by MgGDP observed by others is due to nucleotide binding to the *active* site. The inhibition was observed only at extremely high MgGDP concentrations with a K_i ~11 mM. Such low-affinity binding resulted from binding to the active site after saturation to the high-affinity allosteric site and from antagonistic interactions with substrates. We have shown that a range of high MgADP concentrations inhibits Fru-6-P and that this effect is due to MgADP binding to the active site of the E187A mutant (Figure 4). Johnson and Reinhart also documented the antagonism of the negatively charged Fru-6-P when either MgATP or MgADP occupies the neighboring position within the active site of the wild-type enzyme (*1*). Moreover, Byrnes et al. (*12*) showed in *B. stearothermophilus* PFK that MgGDP activates at low but inhibits at high MgGDP concentrations. The inhibition at high MgGDP concentrations is competitive with MgATP and noncompetitive with Fru-6-P.

Considering that MgADP and MgGDP play rather insignificant roles in other homologous PFK enzymes, the lack of activation by MgADP or MgGDP probably is not surprising. In *B. stearothermophilus*, MgADP barely enhances the binding for Fru-6-P at 25 °C; rather, MgADP binding is inferred from the mitigation of inhibition by PEP toward Fru-6-P. Activation by MgADP becomes apparent only at higher temperatures (*41*). In *Lactobacillus bulgaricus* and *Spiroplasma citri*, wherein an aspartate occupies position 187, MgGDP appears to have virtually no effects on substrate binding (*7*). No experiments have been performed to determine whether MgGDP binds to either of these enzymes.

In summary, we have shown that the binding of MgADP in the E187A mutant of *E. coli* PFK is independent of its allosteric response. MgADP binds to the active and allosteric sites of the mutant enzyme with affinities comparable to those seen in the wild-type counterpart. MgADP at high concentrations noncompetitively inhibits Fru-6-P and competitively inhibits MgATP binding, and MgADP at low concentrations competitively inhibits PEP but does not affect Fru-6-P binding. These findings directly contrast with the classical Monod−Wyman−Changeux two-state model, which requires that effector ligand binding is intrinsically related to allosteric response and that this relationship is manifested through conformational transitions.

REFERENCES

1. Johnson, J. L., and Reinhart, G. D. (1994) *Biochemistry 33*, 2635−2643.
2. Blangy, D., Buc, H., and Monod, J. (1968) *J. Mol. Biol. 31*, 13−35.
3. Johnson, J. L., and Reinhart, G. D. (1992) *Biochemistry 31*, 11510−11518.
4. Shirakihara, Y., and Evans, P. R. (1988) *J. Mol. Biol. 204*, 973−994.
5. Lau, F. T.-K., and Fersht, A. R. (1987) *Nature 326*, 811−812.
6. Lau, F. T.-K., and Fersht, A. R. (1989) *Biochemistry 28*, 6841−6847.
7. Auzat, I., Le Bras, G., Branny, P., De La Torre, F., Theunissen, B., and Garel, J. R. (1994) *J. Mol. Biol. 235*, 68−72.
8. Deville-Bonne, D., Bourgain, F., and Garel, J.-R. (1991) *Biochemistry 30*, 5750−5754.
9. Auzat, I., Byrnes, W. M., Garel, J.-R., and Chang, S. H. (1995) *Biochemistry 34*, 7062−7068.
10. Reinhart, G. D., and Hartleip, S. B. (1987) *Arch. Biochem. Biophys. 258*, 65−76.
11. Evans, P. R. (1992) *Proc. Robert A. Welch Found. Conf. Chem. Res. 36*, 39−54.
12. Byrnes, W. M., Hu, W., Younathan, E. S., and Chang, S. H. (1995) *J. Biol. Chem. 270*, 3828−3835.
13. Lau, F. T.-K., Fersht, A. R., Hellinga, H. W., and Evans, P. R. (1987) *Biochemistry 26*, 4143−4148.
14. Johnson, J. L., and Reinhart, G. D. (1997) *Biochemistry 36*, 12814−12822.
15. Johnson, J. L., and Reinhart, G. D. (1994) *Biochemistry 33*, 2644−2650.
16. Zheng, R.-L., and Kemp, R. G. (1992) *J. Biol. Chem. 267*, 23640−23645.
17. Daldal, J. (1983) *J. Mol. Biol. 168*, 285−305.
18. Sambrook, J., Fritsh, E. F., and Maniatis, T. (1989) in *Molecular Cloning*, 2nd ed., pp 1.74−1.84, Cold Spring Harbor Laboratory Press, Cold Spring Harbor, NY.
19. Kotlarz, D., and Buc, H. (1982) *Methods Enzymol. 90*, 60−70.
20. Hill, A. V. (1910) *J. Physiol. 40*, 4−7.
21. Weber, G. (1952) *Biochemistry 51*, 145−155.
22. Reinhart, G. D., Hartleip, S. B., and Symcox, M. M. (1989) *Proc. Natl. Acad. Sci. U.S.A. 86*, 4032−4036.
23. Symcox, M. M., and Reinhart, G. D. (1992) *Anal. Biochem. 206*, 394−399.
24. Reinhart, G. D. (1983) *Arch. Biochem. Biophys. 224*, 389−401.
25. Reinhart, G. D. (1985) *Biochemistry 24*, 7166−7172.
26. Reinhart, G. D. (1988) *Biophys. Chem. 30*, 159−172.
27. Uyeda, K. (1979) *Adv. Enzymol. Relat. Areas Mol. Biol. 48*, 193−244.

28. Cottam, G. L., and Uyeda, K. (1973) *Arch. Biochem. Biophys. 154*, 683−690.
29. Reinhart, G. D., and Lardy, H. (1980) *Biochemistry 19*, 1484−1490.
30. Reinhart, G. D., and Lardy, H. (1980) *Biochemistry 19*, 1491−1495.
31. Reinhart, G. D. (1981) in *Regulation of Carbohydrate Formation and Utilization in Mammals* (Veneziale, C. M., Ed.) pp 99−119, University Park Press, Baltimore, MD.
32. Schirmer, T., and Evans, P. R. (1990) *Nature 343*, 140−145.
33. Mavis, R. D., and Stellwagen, E. (1970) *J. Biol. Chem. 245*, 674−680.
34. Le Bras, G., and Garel, J.-R. (1982) *Biochemistry 21*, 6656−6660.
35. Teschner, W., and Garel, J.-R. (1989) *Biochemistry 28*, 1912−1916.
36. Pham, A. S., and Reinhart, G. D. (2001) *J. Biol. Chem.* (submitted for publication).
37. Reinhart, G. D., and Lardy, H. (1980) *Biochemistry 19*, 1477−1484.
38. Monod, J., Wyman, J., and Changeux, J. P. (1965) *J. Mol. Biol. 12*, 88−118.
39. Pham, A. S., and Reinhart, G. D. (2001) *Biochemistry 40*, 4150−4158.
40. Deville-Bonne, D., and Garel, J.-R. (1992) *Biochemistry 31*, 1695−1700.
41. Braxton, B. L., Tlapak-Simmons, V. L., and Reinhart, G. D. (1994) *J. Biol. Chem. 269*, 47−50.

BI001768Z